First-principles calculation of higher-order elastic constants using exact deformation-gradient tensors

S. P. Łepkowski

Institute of High Pressure Physics - Unipress, Polish Academy of Sciences, ul. Sokołowska 29/37, 01-142 Warszawa, Poland

(Received 12 June 2020; revised 18 September 2020; accepted 8 October 2020; published 23 October 2020)

We propose a general and easy-to-use method of the *ab initio* calculation of the higher-order elastic constants, which is based on the analytical formulas for the deformation-gradient tensors as functions of the Lagrangian strain. The method allows for elimination of the truncation errors in the Taylor expansion series of the deformation gradients and is particularly useful to calculate the fourth-order elastic constants, where large strains have to be applied. It also facilitates the calculation of the Lagrangian stress, which is helpful in determination of the strain-stress relations. To demonstrate the application of our approach, we derive the analytic formulas for the deformation gradients as functions of the Lagrangian strain tensors, which are used in calculations of the third-order elastic constants in trigonal crystals and the fourth-order elastic constants in cubic crystals. Then, we perform the *ab initio* calculations of the fourth-order elastic constants in face-centered-cubic aluminum. We discuss the results obtained using the strain-energy and strain-stress relations and analyze the errors of the fourth-order elastic constants which would be incurred when approximating the deformation gradients by the Taylor polynomials. We show that the relatively small truncation errors in the Taylor expansion series of the deformation gradients can cause significant deviations of the fourth-order elastic constants. This effect is larger for the strain-energy method than for the strain-stress approach. We find that in both methods, the deviations are particularly significant for the C_{1155}, C_{1266}, C_{4455}, C_{1255}, and C_{1456} elastic constants and are mainly caused by the truncation errors in the nondiagonal elements of the Taylor expansion series of the deformation gradients.

DOI: 10.1103/PhysRevB.102.134116

I. INTRODUCTION

In the continuum elasticity theory, the elastic constants provide a complete description of the elastic response of a solid [1]. The second-order elastic constants (SOECs) determine harmonic properties of materials and are used in the linear strain theory when the crystal energy can be accurately expressed to the second order in the strain, leading to the linear relationships between strains and stresses. As the applied deformations increase, the higher-order terms in the strain start to contribute significantly to the crystal energy and the nonlinear elasticity theory should be considered [1]. Anharmonicity of the crystal lattice is described by the higher-order elastic constants (HOECs) and is crucial for determination of many physical properties of solids, including thermal expansion, thermal conductivity, and electron-phonon and phonon-phonon interactions [1–3]. In particular, the HOECs play an important role in estimation of the generalized Grüneisen parameters, the pressure dependence of the SOECs, the intrinsic mechanical strength, and ductility of materials [4–8]. Furthermore, the third-order elastic constants (TOECs), which are the lowest order of the HOECs, are often applied to describe the nonlinear mechanical effects in nanoscale materials [9–14]. The fourth-order elastic constants (FOECs) increase the accuracy of the description of the nonlinear elasticity phenomena and are particularly important in determination of the structural phase transitions at high pressures and finite deformations [15–17].

The HOECs can be determined experimentally using ultrasonic velocity measurements or theoretically from atomistic calculations. The experimental methods rely on the measurements of the changes in acoustic velocities under hydrostatic and uniaxial stresses [18,19]. These experiments are difficult and usually generate large uncertainties in the obtained results. The difficulties increase with the order of the HOECs and for the FOECs, there are only few materials for which some experimental values are available [15]. The computational methods based on first-principles calculations are a feasible alternative for predicting the HOECs in crystalline solids. They combine the approach of the finite homogeneous deformations of supercells with the quantum-mechanical calculations of the total energy and the stresses [20–28]. The Lagrangian strain formalism is usually used to determine the HOECs from either the strain-energy or the strain-stress dependencies. This approach was initially used to obtain the TOECs and then was extended for the FOECs [15,21].

In order to obtain the full set of the HOECs from the first-principles calculations, one has to apply different types of the Lagrangian strain [20–27]. For each type of strain, a series of deformed supercells is constructed using the deformation-gradient tensors. The deformation gradients have commonly been obtained by truncating an infinite Taylor expansion series

in the Lagrangian strain [22–26]. The approximating Taylor polynomials have usually been taken of the third or fourth order and the influence of the truncation errors on the HOECs have never been discussed. A different approach has recently been proposed in the work of Tanner *et al.* [28], where the particular types of the deformation gradients have been proposed via determination of the suitable branches of the infinitesimal strain tensors. This method leads the complex forms of the Lagrangian strain, which result in long equations for the stresses and the free energy, even in the case of the TOECs in cubic crystals [28].

In this work, we propose a general and easy-to-use method of the *ab initio* calculation of the HOECs, which is based on the analytical formulas for the deformation-gradient tensors as functions of the Lagrangian strain. The method allows for elimination of the truncation errors in the Taylor expansion series of the deformation gradients and is particularly useful to calculate the FOECs, where large strains have to be applied. It also facilitates the calculation of the Lagrangian stress, which is helpful in determination of the strain-stress relations. To demonstrate the application of our approach, we derive the analytic formulas for the deformation gradients as functions of the Lagrangian strain tensors, which are used in calculations of the TOECs in trigonal crystals and the FOECs in cubic crystals. Then, we perform the *ab initio* calculations of the FOECs in face-centered-cubic aluminum (fcc Al). We discuss the results obtained using the strain-energy and strain-stress methods and analyze the errors of the FOECs which would be incurred when approximating the deformation gradients by the Taylor polynomials. We show that the relatively small truncation errors in the Taylor expansion series of the deformation gradients can cause significant deviations of the FOECs, which makes our exact analytical formulas for the deformation gradients important.

II. THEORETICAL METHOD

In the theory of nonlinear elasticity, local deformation of a solid body is described by the deformation-gradient tensor $\boldsymbol{J}$, which is defined by the Jacobian matrix

$$J_{\alpha\beta} = \frac{\partial x_\alpha}{\partial a_\beta}, \tag{1}$$

where a_β and x_α are the coordinates of a point in the undeformed and deformed configurations, respectively [1]. The deformation gradient is generally a nonsymmetric matrix since it takes into account a rigid rotation of a deformed body. Using $\boldsymbol{J}$, we define Lagrangian strain tensor $\boldsymbol{\eta}$ as

$$\boldsymbol{\eta} = \tfrac{1}{2}(\boldsymbol{J}^T\boldsymbol{J} - \boldsymbol{I}), \tag{2}$$

where $\boldsymbol{I}$ is the 3×3 identity matrix. The Lagrangian strain is a symmetric matrix and therefore, it is a rotation-independent quantity. It is convenient to represent $\boldsymbol{\eta}$ in the Voigt convention as a six-dimensional vector ($\eta_{11} \rightarrow \eta_1$, $\eta_{22} \rightarrow \eta_2$, $\eta_{33} \rightarrow \eta_3$, $\eta_{23} \rightarrow \eta_4/2$, $\eta_{13} \rightarrow \eta_5/2$, $\eta_{12} \rightarrow \eta_6/2$). The elastic constants are defined by expanding the free-energy density, $\rho_0 E$, as a Taylor series in strain,

$$\rho_0 E(\boldsymbol{\eta}) = \rho_0 E(0) + \frac{1}{2!}\sum_{i,j=1}^{6} C_{ij}\eta_i\eta_j + \frac{1}{3!}\sum_{i,j,k=1}^{6} C_{ijk}\eta_i\eta_j\eta_k + \frac{1}{4!}\sum_{i,j,k,l=1}^{6} C_{ijkl}\eta_i\eta_j\eta_k\eta_l + \cdots, \tag{3}$$

where E is the Helmholtz free energy per unit mass, ρ_0 is the mass density of the unstrained material, and C_{ij}, C_{ijk}, and C_{ijkl} are the SOECs, the TOECs, and the FOECs, respectively. The Lagrangian stress is defined as the first-order derivative of $\rho_0 E$, with respect to the Lagrangian strain,

$$t_i = \rho_0\frac{\partial E}{\partial \eta_i} = \frac{1}{2!}\sum_{j=1}^{6} C_{ij}\eta_j + \frac{1}{3!}\sum_{j,k=1}^{6} C_{ijk}\eta_j\eta_k + \frac{1}{4!}\sum_{j,k,l=1}^{6} C_{ijkl}\eta_j\eta_k\eta_l + \cdots, \tag{4}$$

where the Voight convention is used for the Lagrangian stress tensor ($t_{11} \rightarrow t_1$, $t_{22} \rightarrow t_2$, $t_{33} \rightarrow t_3$, $t_{23} \rightarrow t_4$, $t_{13} \rightarrow t_5$, $t_{12} \rightarrow t_6$). The tensor of Lagrangian stress $\boldsymbol{t}$ is related to the Cauchy stress $\boldsymbol{\sigma}$ and the deformation gradient $\boldsymbol{J}$ via the following formula:

$$\boldsymbol{t} = \det(\boldsymbol{J})\boldsymbol{J}^{-1}\boldsymbol{\sigma}(\boldsymbol{J}^T)^{-1}. \tag{5}$$

In general, the first-principles calculations provide the free-energy density and the Cauchy stress tensor for deformed crystal supercells, which are used to determine the elastic constants either from Eq. (3) or from Eqs. (4) and (5) [26–28]. Homogeneous deformations are applied using the matrices $\boldsymbol{J}$, which transform the crystal lattice vectors from the unstrained configuration r_i to the strained configurations r'_i:

$$r'_i = J_{ij}r_j. \tag{6}$$

In order to perform the *ab initio* calculations of the HOECs, it is convenient to determine the deformation gradient $\boldsymbol{J}$ from the Lagrangian strain $\boldsymbol{\eta}$, which can be obtained by inverting Eq. (2) [22–26]. In general, for a given $\boldsymbol{\eta}$, the matrix $\boldsymbol{J}$ is not unique and the various solutions differ from one another by a rigid rotation. The lack of a one-to-one transformation between $\boldsymbol{J}$ and $\boldsymbol{\eta}$ is not a concern since the free energy and stresses are invariant under rigid rotations and the deformation gradient for the system without rotation, $\tilde{\boldsymbol{J}}$, is normally considered. Since $\tilde{\boldsymbol{J}} = \tilde{\boldsymbol{J}}^T$, we get from Eq. (2) that

$$\boldsymbol{\eta} = \tfrac{1}{2}(\tilde{\boldsymbol{J}}^2 - \boldsymbol{I}). \tag{7}$$

Note that expressing $\tilde{\boldsymbol{J}}$ in terms of the infinitesimal strain, $\tilde{\boldsymbol{J}} = \boldsymbol{\varepsilon} + \boldsymbol{I}$, one obtains the well-known matrix relation $\boldsymbol{\eta} = \boldsymbol{\varepsilon} + \frac{1}{2}\boldsymbol{\varepsilon}^2$, which was used in Ref. [28] to obtain the strains $\boldsymbol{\eta}$ for the given tensors $\boldsymbol{\varepsilon}$. As we have mentioned in the Introduction, such an approach leads to complex forms of the strains $\boldsymbol{\eta}$ and thus it is difficult to apply to the FOECs. Therefore, in the case of the calculations of the FOECs, Eq. (7) is inverted, as follows:

$$\tilde{\boldsymbol{J}} = (2\boldsymbol{\eta} + \boldsymbol{I})^{1/2}. \tag{8}$$

TABLE I. The types of the strain tensors and the corresponding deformation-gradient tensors for 14 types of strains used to calculate the TOECs in trigonal crystals.

Strain	Deformation gradient	Strain-dependent elements
$\boldsymbol{\eta}_A = \begin{bmatrix} \eta & 0 & 0 \\ 0 & 0 & 0 \\ 0 & 0 & 0 \end{bmatrix}$	$\tilde{J}_A = \begin{bmatrix} \alpha_A & 0 & 0 \\ 0 & 1 & 0 \\ 0 & 0 & 1 \end{bmatrix}$	$\alpha_A = \sqrt{1+2\eta}$
$\boldsymbol{\eta}_B = \begin{bmatrix} \eta & 0 & 0 \\ 0 & \eta & 0 \\ 0 & 0 & 0 \end{bmatrix}$	$\tilde{J}_B = \begin{bmatrix} \alpha_B & 0 & 0 \\ 0 & \alpha_B & 0 \\ 0 & 0 & 1 \end{bmatrix}$	$\alpha_B = \alpha_A$
$\boldsymbol{\eta}_C = \begin{bmatrix} 0 & 0 & 0 \\ 0 & \eta & 0 \\ 0 & 0 & 0 \end{bmatrix}$	$\tilde{J}_C = \begin{bmatrix} 1 & 0 & 0 \\ 0 & \alpha_C & 0 \\ 0 & 0 & 1 \end{bmatrix}$	$\alpha_C = \alpha_A$
$\boldsymbol{\eta}_D = \begin{bmatrix} \eta & 0 & 0 \\ 0 & 0 & \eta \\ 0 & \eta & 0 \end{bmatrix}$	$\tilde{J}_D = \begin{bmatrix} \alpha_D & 0 & 0 \\ 0 & \beta_D & \gamma_D \\ 0 & \gamma_D & \beta_D \end{bmatrix}$	$\alpha_D = \alpha_A$
		$\beta_D = \frac{1}{2}(\sqrt{1+2\eta} + \sqrt{1-2\eta})$
		$\gamma_D = \frac{1}{2}(\sqrt{1+2\eta} - \sqrt{1-2\eta})$
$\boldsymbol{\eta}_E = \begin{bmatrix} 0 & 0 & 0 \\ 0 & 0 & 0 \\ 0 & 0 & \eta \end{bmatrix}$	$\tilde{J}_E = \begin{bmatrix} 1 & 0 & 0 \\ 0 & 1 & 0 \\ 0 & 0 & \alpha_E \end{bmatrix}$	$\alpha_E = \alpha_A$
$\boldsymbol{\eta}_F = \begin{bmatrix} 0 & 0 & 0 \\ 0 & \eta & 0 \\ 0 & 0 & \eta \end{bmatrix}$	$\tilde{J}_F = \begin{bmatrix} 1 & 0 & 0 \\ 0 & \alpha_F & 0 \\ 0 & 0 & \alpha_F \end{bmatrix}$	$\alpha_F = \alpha_A$
$\boldsymbol{\eta}_G = \begin{bmatrix} 0 & 0 & 0 \\ 0 & 0 & \eta \\ 0 & \eta & 0 \end{bmatrix}$	$\tilde{J}_G = \begin{bmatrix} 1 & 0 & 0 \\ 0 & \alpha_G & \beta_G \\ 0 & \beta_G & \alpha_G \end{bmatrix}$	$\alpha_G = \beta_D$
		$\beta_G = \gamma_D$
$\boldsymbol{\eta}_H = \begin{bmatrix} 0 & \eta & 0 \\ \eta & 0 & 0 \\ 0 & 0 & \eta \end{bmatrix}$	$\tilde{J}_H = \begin{bmatrix} \alpha_H & \beta_H & 0 \\ \beta_H & \alpha_H & 0 \\ 0 & 0 & \gamma_H \end{bmatrix}$	$\alpha_H = \beta_D$
		$\beta_H = \gamma_D$
		$\gamma_H = \alpha_A$
$\boldsymbol{\eta}_I = \begin{bmatrix} 0 & 0 & 0 \\ 0 & \eta & \eta \\ 0 & \eta & 0 \end{bmatrix}$	$\tilde{J}_I = \begin{bmatrix} 1 & 0 & 0 \\ 0 & \alpha_I & \beta_I \\ 0 & \beta_I & \gamma_I \end{bmatrix}$	$\alpha_I = \frac{5-\sqrt{5}}{10}\sqrt{1+\eta(1-\sqrt{5})} + \frac{5+\sqrt{5}}{10}\sqrt{1+\eta(1+\sqrt{5})}$
		$\beta_I = \frac{1}{\sqrt{5}}(\sqrt{1+\eta(1+\sqrt{5})} - \sqrt{1+\eta(1-\sqrt{5})})$
		$\gamma_I = \frac{5+\sqrt{5}}{10}\sqrt{1+\eta(1-\sqrt{5})} + \frac{5-\sqrt{5}}{10}\sqrt{1+\eta(1+\sqrt{5})}$
$\boldsymbol{\eta}_J = \begin{bmatrix} 0 & 0 & \eta \\ 0 & \eta & 0 \\ \eta & 0 & 0 \end{bmatrix}$	$\tilde{J}_J = \begin{bmatrix} \alpha_J & 0 & \beta_J \\ 0 & \gamma_J & 0 \\ \beta_J & 0 & \alpha_J \end{bmatrix}$	$\alpha_J = \beta_D$
		$\beta_J = \gamma_D$
		$\gamma_J = \alpha_A$
$\boldsymbol{\eta}_K = \begin{bmatrix} \eta & 0 & 0 \\ 0 & \eta & 0 \\ 0 & 0 & \eta \end{bmatrix}$	$\tilde{J}_K = \begin{bmatrix} \alpha_K & 0 & 0 \\ 0 & \alpha_K & 0 \\ 0 & 0 & \alpha_K \end{bmatrix}$	$\alpha_K = \alpha_A$
$\boldsymbol{\eta}_L = \begin{bmatrix} 0 & 0 & \eta \\ 0 & 0 & 0 \\ \eta & 0 & \eta \end{bmatrix}$	$\tilde{J}_L = \begin{bmatrix} \gamma_L & 0 & \beta_L \\ 0 & 1 & 0 \\ \beta_L & 0 & \alpha_L \end{bmatrix}$	$\alpha_L = \alpha_I$
		$\beta_L = \beta_I$
		$\gamma_L = \gamma_I$

TABLE I. (*Continued.*)

Strain	Deformation gradient	Strain-dependent elements
$\boldsymbol{\eta}_M = \begin{bmatrix} \eta & 0 & 0 \\ 0 & 0 & \eta \\ 0 & \eta & \eta \end{bmatrix}$	$\tilde{J}_M = \begin{bmatrix} \delta_M & 0 & 0 \\ 0 & \gamma_M & \beta_M \\ 0 & \beta_M & \alpha_M \end{bmatrix}$	$\alpha_M = \alpha_I$
		$\beta_M = \beta_I$
		$\gamma_M = \gamma_I$
		$\delta_M = \alpha_A$
$\boldsymbol{\eta}_N = \begin{bmatrix} \eta & 0 & \eta \\ 0 & \eta & 0 \\ \eta & 0 & 0 \end{bmatrix}$	$\tilde{J}_N = \begin{bmatrix} \alpha_N & 0 & \beta_N \\ 0 & \delta_N & 0 \\ \beta_N & 0 & \gamma_N \end{bmatrix}$	$\alpha_N = \alpha_I$
		$\beta_N = \beta_I$
		$\gamma_N = \gamma_I$
		$\delta_N = \alpha_A$

Then, the right-hand side of Eq. (8) can be expanded as a Taylor series in strain,

$$\tilde{\boldsymbol{J}} = \boldsymbol{I} + \boldsymbol{\eta} + \sum_{m=2}^{\infty} C_m \boldsymbol{\eta}^m, \tag{9}$$

where the C_m coefficients are given by the following recurrence relation:

$$C_m = \begin{cases} \frac{3-2m}{m} C_{m-1}, & m > 2 \\ -\frac{1}{2}, & m = 2 \end{cases}. \tag{10}$$

Commonly, the deformation gradient $\tilde{\boldsymbol{J}}$ has been approximated by truncating the Taylor series in Eqs. (9) and (10) to three or four terms [22–26]. In this work, we propose to compute analytically the matrix square root occurring in Eq. (8), which allows for elimination of the truncation error while using a Taylor series given by Eqs. (9) and (10). Since $\boldsymbol{\eta}$ is a real and symmetric matrix, the matrix $2\boldsymbol{\eta} + \boldsymbol{I}$ is a diagonalizable and thus it can be represented as follows:

$$2\boldsymbol{\eta} + \boldsymbol{I} = \boldsymbol{V}\boldsymbol{D}\boldsymbol{V}^{-1}, \tag{11}$$

where $\boldsymbol{D}$ is a diagonal matrix with the eigenvalues as the diagonal elements and $\boldsymbol{V}$ is an orthogonal matrix with the eigenvectors as columns. Combing Eqs. (8) and (11), we get

$$\tilde{\boldsymbol{J}} = \boldsymbol{V}(\boldsymbol{D})^{1/2}\boldsymbol{V}^{-1}, \tag{12}$$

which provides the exact deformation-gradient tensor for a given $\boldsymbol{\eta}$. Having the analytic formula for $\tilde{\boldsymbol{J}}$, it is convenient to introduce a 6×6 matrix $\boldsymbol{S}$, which determines the relationship between tensors $\boldsymbol{t}$ and $\boldsymbol{\sigma}$ in the Voigt configuration, according to Eq. (5),

$$\boldsymbol{t} = \boldsymbol{S}\boldsymbol{\sigma} = \det(\tilde{\boldsymbol{J}})\tilde{\boldsymbol{J}}^{-1}\boldsymbol{\sigma}(\tilde{\boldsymbol{J}}^{T})^{-1}. \tag{13}$$

Note that the matrix $\boldsymbol{S}$ is uniquely determined by the tensor $\boldsymbol{\eta}$ since there is a one-to-one transformation between $\tilde{\boldsymbol{J}}$ and $\boldsymbol{\eta}$.

III. APPLICATION

In order to demonstrate the application of the method presented above, we derive the analytic formulas for the tensors $\tilde{\boldsymbol{J}}$ as functions of the tensors $\boldsymbol{\eta}$, which are used in calculations of the TOECs in trigonal crystals and the FOECs in cubic crystals. Since the obtained tensors $\tilde{\boldsymbol{J}}$ are particularly useful when large strains have to be applied, we then focus on the FOECs and calculate their values for fcc Al.

A. TOEC in trigonal crystals and FOEC in cubic crystals

In trigonal crystals, we have 14 independent TOECs and thus 14 types of strains are applied to calculate the TOECs using the strain-energy method [22]. In cubic crystals, the set of FOECs consists of 11 elements and 11 types of strains are sufficient to determine all the FOECs using the strain-energy method [15]. In Tables I and II, we present the types of strains and the corresponding tensors $\tilde{\boldsymbol{J}}$, which are used to calculate the TOECs in trigonal crystals and the FOECs in cubic crystals, respectively [15,22]. In both cases, all the tensors $\boldsymbol{\eta}$ depend on only one parameter η. The obtained tensors $\tilde{\boldsymbol{J}}$ are valid when the radicands occurring in the expressions for the elements of $\tilde{\boldsymbol{J}}$ are non-negative. Thus, we find that $\eta \in [\frac{1-\sqrt{5}}{4}, \frac{1}{2}]$ for the TOECs in trigonal crystals and $\eta \in [\frac{1-\sqrt{2}}{2}, \frac{1}{2}]$ for the FOECs in cubic crystals.

B. FOEC in fcc aluminum

To illustrate the utility of using the analytic formulas for the $\tilde{\boldsymbol{J}}$ tensors, we focus on the FOECs in cubic crystals since in determination of the FOECs, larger strains should be involved than in the case of the TOECs and thus, the advantage of using our method over the approach based on the Taylor expansion series of the $\tilde{\boldsymbol{J}}$ tensors is more pronounced. The FOECs were calculated for several cubic materials including fcc metals (Cu, Al, Au, Ag), body-centered-cubic W, and rocksalt MgO, whereas there is no single set of the FOECs known experimentally so far [15,16,25]. Here, we choose fcc Al, which was one of four metals studied theoretically in Ref. [15].

We use 11 types of strains, which are listed in Table II. In every case, the parameter η is varied between $-\eta_{\max}$ and $\eta_{\max}$ with step $\Delta\eta_{\max} = 0.0025$. The parameter $\eta_{\max}$ determines the range of the applied strain to the unit cell and affects the contribution of the FOECs to the free energy and the stresses.

TABLE II. The types of the strain tensors and the corresponding deformation-gradient tensors for 11 types of strains used to calculate the FOECs in cubic crystals.

Strain	Deformation gradient	Strain-dependent elements
$\boldsymbol{\eta}_A = \begin{bmatrix} \eta & 0 & 0 \\ 0 & 0 & 0 \\ 0 & 0 & 0 \end{bmatrix}$	$\tilde{J}_A = \begin{bmatrix} \alpha_A & 0 & 0 \\ 0 & 1 & 0 \\ 0 & 0 & 1 \end{bmatrix}$	$\alpha_A = \sqrt{1+2\eta}$
$\boldsymbol{\eta}_B = \begin{bmatrix} \eta & 0 & 0 \\ 0 & \eta & 0 \\ 0 & 0 & 0 \end{bmatrix}$	$\tilde{J}_B = \begin{bmatrix} \alpha_B & 0 & 0 \\ 0 & \alpha_B & 0 \\ 0 & 0 & 1 \end{bmatrix}$	$\alpha_B = \alpha_A$
$\boldsymbol{\eta}_C = \begin{bmatrix} \eta & 0 & 0 \\ 0 & -\eta & 0 \\ 0 & 0 & 0 \end{bmatrix}$	$\tilde{J}_C = \begin{bmatrix} \alpha_C & 0 & 0 \\ 0 & \beta_C & 0 \\ 0 & 0 & 1 \end{bmatrix}$	$\alpha_C = \alpha_A$ $\beta_C = \sqrt{1-2\eta}$
$\boldsymbol{\eta}_D = \begin{bmatrix} \eta & 0 & 0 \\ 0 & 0 & \eta \\ 0 & \eta & 0 \end{bmatrix}$	$\tilde{J}_D = \begin{bmatrix} \alpha_D & 0 & 0 \\ 0 & \beta_D & \gamma_D \\ 0 & \gamma_D & \beta_D \end{bmatrix}$	$\alpha_D = \alpha_A$ $\beta_D = \frac{1}{2}(\sqrt{1+2\eta} + \sqrt{1-2\eta})$ $\gamma_D = \frac{1}{2}(\sqrt{1+2\eta} - \sqrt{1-2\eta})$
$\boldsymbol{\eta}_E = \begin{bmatrix} \eta & \eta & 0 \\ \eta & 0 & 0 \\ 0 & 0 & 0 \end{bmatrix}$	$\tilde{J}_E = \begin{bmatrix} \alpha_E & \beta_E & 0 \\ \beta_E & \gamma_E & 0 \\ 0 & 0 & 1 \end{bmatrix}$	$\alpha_E = \frac{5-\sqrt{5}}{10}\sqrt{1+\eta(1-\sqrt{5})} + \frac{5+\sqrt{5}}{10}\sqrt{1+\eta(1+\sqrt{5})}$ $\beta_E = \frac{1}{\sqrt{5}}(\sqrt{1+\eta(1+\sqrt{5})} - \sqrt{1+\eta(1-\sqrt{5})})$ $\gamma_E = \frac{5+\sqrt{5}}{10}\sqrt{1+\eta(1-\sqrt{5})} + \frac{5-\sqrt{5}}{10}\sqrt{1+\eta(1+\sqrt{5})}$
$\boldsymbol{\eta}_F = \begin{bmatrix} 0 & \eta & \eta \\ \eta & 0 & \eta \\ \eta & \eta & 0 \end{bmatrix}$	$\tilde{J}_F = \begin{bmatrix} \alpha_F & \beta_F & \beta_F \\ \beta_F & \alpha_F & \beta_F \\ \beta_F & \beta_F & \alpha_F \end{bmatrix}$	$\alpha_F = \frac{1}{3}(\sqrt{1+4\eta} + 2\sqrt{1-2\eta})$ $\beta_F = \frac{1}{3}(\sqrt{1+4\eta} - \sqrt{1-2\eta})$
$\boldsymbol{\eta}_G = \begin{bmatrix} 0 & 0 & 0 \\ 0 & 0 & \eta \\ 0 & \eta & 0 \end{bmatrix}$	$\tilde{J}_G = \begin{bmatrix} 1 & 0 & 0 \\ 0 & \alpha_G & \beta_G \\ 0 & \beta_G & \alpha_G \end{bmatrix}$	$\alpha_G = \beta_D$ $\beta_G = \gamma_D$
$\boldsymbol{\eta}_H = \begin{bmatrix} \eta & \eta & 0 \\ \eta & \eta & 0 \\ 0 & 0 & 0 \end{bmatrix}$	$\tilde{J}_H = \begin{bmatrix} \alpha_H & \beta_H & 0 \\ \beta_H & \alpha_H & 0 \\ 0 & 0 & 1 \end{bmatrix}$	$\alpha_H = \frac{1}{2}(\sqrt{1+4\eta} + 1)$ $\beta_H = \frac{1}{2}(\sqrt{1+4\eta} - 1)$
$\boldsymbol{\eta}_I = \begin{bmatrix} \eta & 0 & 0 \\ 0 & \eta & \eta \\ 0 & \eta & 0 \end{bmatrix}$	$\tilde{J}_I = \begin{bmatrix} \alpha_I & 0 & 0 \\ 0 & \beta_I & \gamma_I \\ 0 & \gamma_I & \delta_I \end{bmatrix}$	$\alpha_I = \alpha_A$ $\beta_I = \alpha_E$ $\gamma_I = \beta_E$ $\delta_I = \gamma_E$
$\boldsymbol{\eta}_J = \begin{bmatrix} \eta & \eta & \eta \\ \eta & 0 & \eta \\ \eta & \eta & 0 \end{bmatrix}$	$\tilde{J}_J = \begin{bmatrix} \alpha_J & \beta_J & \beta_J \\ \beta_J & \gamma_J & \delta_J \\ \beta_J & \delta_J & \gamma_J \end{bmatrix}$	$\alpha_J = \frac{1}{2}(\sqrt{1+2\eta(1+\sqrt{2})} + \sqrt{1+2\eta(1-\sqrt{2})})$ $\beta_J = \frac{1}{2\sqrt{2}}(\sqrt{1+2\eta(1+\sqrt{2})} - \sqrt{1+2\eta(1-\sqrt{2})})$ $\gamma_J = \frac{1}{4}(\sqrt{1+2\eta(1+\sqrt{2})} + \sqrt{1+2\eta(1-\sqrt{2})} + 2\sqrt{1-2\eta})$ $\delta_J = \frac{1}{4}(\sqrt{1+2\eta(1+\sqrt{2})} + \sqrt{1+2\eta(1-\sqrt{2})} - 2\sqrt{1-2\eta})$
$\boldsymbol{\eta}_K = \begin{bmatrix} \eta & 0 & 0 \\ 0 & \eta & 0 \\ 0 & 0 & \eta \end{bmatrix}$	$\tilde{J}_K = \begin{bmatrix} \alpha_K & 0 & 0 \\ 0 & \alpha_K & 0 \\ 0 & 0 & \alpha_K \end{bmatrix}$	$\alpha_K = \alpha_A$

For small $\eta_{\max}$, this contribution is small in comparison to the contribution coming from the SOECs and the TOECs, while for large $\eta_{\max}$, the fifth- and sixth-order elastic constants come into play [15,28]. We choose the optimal $\eta_{\max} = 0.11$ for determination of the FOECs in fcc Al by the strain-energy and strain-stress methods. Note that $\eta_{\max} < \frac{\sqrt{2}-1}{2}$ and thus, the formulas for the $\tilde{\boldsymbol{J}}$ tensors, listed in Table II, can be used.

For each $\boldsymbol{\eta}$, the free-energy density $\rho_0 E$ and the elements of the tensor $\boldsymbol{t}$ are polynomial functions of a single parameter

TABLE III. The fourth-degree coefficients in the strain-energy relation [Eq. (3)] and the third-degree coefficients in the strain-stress relations [Eq. (4)] for 11 types of the strain tensors (the Voight convention) used to calculate the FOECs in cubic crystals.

Strain types	Fourth-degree coefficients in the strain-energy relation	Third-degree coefficients in the strain-stress relations
$\boldsymbol{\eta}_A = (\eta, 0, 0, 0, 0, 0)$	$\frac{1}{24}C_{1111}$	$t_1(\eta):\ \frac{1}{6}C_{1111}$
		$t_2(\eta):\ \frac{1}{6}C_{1112}$
$\boldsymbol{\eta}_B = (\eta, \eta, 0, 0, 0, 0)$	$\frac{1}{12}C_{1111} + \frac{1}{3}C_{1112} + \frac{1}{4}C_{1122}$	$t_1(\eta):\ \frac{1}{6}C_{1111} + \frac{2}{3}C_{1112} + \frac{1}{2}C_{1122}$
		$t_3(\eta):\ \frac{1}{3}C_{1112} + C_{1123}$
$\boldsymbol{\eta}_C = (\eta, -\eta, 0, 0, 0, 0)$	$\frac{1}{12}C_{1111} - \frac{1}{3}C_{1112} + \frac{1}{4}C_{1122}$	
$\boldsymbol{\eta}_D = (\eta, 0, 0, 2\eta, 0, 0)$	$\frac{1}{24}C_{1111} + C_{1144} + \frac{2}{3}C_{4444}$	$t_1(\eta):\ \frac{1}{6}C_{1111} + 2C_{1144}$
$\boldsymbol{\eta}_E = (\eta, 0, 0, 0, 0, 2\eta)$	$\frac{1}{24}C_{1111} + C_{1155} + \frac{2}{3}C_{4444}$	$t_1(\eta):\ \frac{1}{6}C_{1111} + 2C_{1155}$
		$t_2(\eta):\ \frac{1}{6}C_{1112} + 2C_{1266}$
		$t_3(\eta):\ \frac{1}{6}C_{1112} + 2C_{1255}$
$\boldsymbol{\eta}_F = (0, 0, 0, 2\eta, 2\eta, 2\eta)$	$2C_{4444} + 12C_{4455}$	$t_1(\eta):\ 8C_{1456}$
		$t_4(\eta):\ \frac{4}{3}C_{4444} + 8C_{4455}$
$\boldsymbol{\eta}_G = (0, 0, 0, 2\eta, 0, 0)$	$\frac{2}{3}C_{4444}$	$t_4(\eta):\ \frac{4}{3}C_{4444}$
$\boldsymbol{\eta}_H = (\eta, \eta, 0, 0, 0, 2\eta)$	$\frac{1}{12}C_{1111} + \frac{1}{3}C_{1112} + \frac{1}{4}C_{1122} + 2C_{1155} + 2C_{1266} + \frac{2}{3}C_{4444}$	
$\boldsymbol{\eta}_I = (\eta, \eta, 0, 2\eta, 0, 0)$	$\frac{1}{12}C_{1111} + \frac{1}{3}C_{1112} + \frac{1}{4}C_{1122} + C_{1144} + C_{1155} + 2C_{1255} + \frac{2}{3}C_{4444}$	
$\boldsymbol{\eta}_J = (\eta, 0, 0, 2\eta, 2\eta, 2\eta)$	$\frac{1}{24}C_{1111} + C_{1144} + 2C_{1155} + 8C_{1456} + 2C_{4444} + 12C_{4455}$	
$\boldsymbol{\eta}_K = (\eta, \eta, \eta, 0, 0, 0)$	$\frac{1}{8}C_{1111} + C_{1112} + \frac{3}{4}C_{1122} + \frac{3}{2}C_{1123}$	

η, according to Eqs. (3) and (4). The values of the FOECs are calculated from the coefficients of the third- and fourth-degree terms in the case of the strain-stress method and the strain-energy approach, respectively. These coefficients are expressed by the linear combinations of the FOECs and we present them in Table III. In Appendix A, we present the $\boldsymbol{S}$ matrices for six types of deformations, i.e., $\boldsymbol{\eta}_A$, $\boldsymbol{\eta}_B$, $\boldsymbol{\eta}_D$, $\boldsymbol{\eta}_E$, $\boldsymbol{\eta}_F$, and $\boldsymbol{\eta}_G$, which are used in the strain-stress method. In Appendix B, we show how the TOECs and the SOECs can be obtained using the method of least squares.

The calculations of the total energy and the Cauchy stress tensor have been carried out using the VASP package which is a plane-wave pseudopotential implementation of the density functional theory [29,30]. For the exchange-correlation functional, the generalized gradient approximation with the Perdew-Burke-Ernzerhof approach has been used [31]. The Brillouin-zone integrals have been calculated using $35\times35\times35$ Monkhorst-Pack mesh and a cutoff energy for the plane-wave basis set has been chosen to be equal to 600 eV. The values of the k-point mesh size and the cutoff energy are slightly larger than those used in Ref. [15].

First, we discuss the results obtained using the analytic formulas for the $\tilde{\boldsymbol{J}}$ tensors. In Fig. 1, we show the calculated dependencies of the $\rho_0 E$ on the parameter η which are used to determine the FOECs in the strain-energy method (see Table III). In Fig. 2, we present the changes in the selected elements of the tensors $\boldsymbol{t}$ as functions of η which are employed in the strain-stress method (see Table III). In these figures, symbols correspond to the calculated *ab initio* data while the solid lines represent the fourth- and third-order polynomial fits. Note that for a clear illustration of the *ab initio* results, we only show every fourth computed data point.

In Table IV(a), we present the calculated FOECs, while the SOECs and the TOECs are show in Table IV(b). In Table IV, we include the experimental results for the SOECs and the TOECs taken from Refs. [32–34] and the theoretical results for the SOECs, the TOECs, and the FOECs obtained in Ref. [15] using the strain-energy method. We observe that our SOECs agree very well with the experimental results presented in the literature. The TOECs obtained using the strain-stress method show also good agreement with the measured TOECs while some discrepancies are observed between the calculated TOECs using the strain-energy method and the experimental results. A similar situation has recently been reported for the TEOCs in diamond [26]. Finally, we notice that our FOECs obtained using the strain-energy and strain-stress methods are consistent with the theoretical results presented in Ref. [15].

Now, we compare the results obtained using the exact the $\tilde{\boldsymbol{J}}$ tensors and their Taylor series approximations. To this end, we discuss the truncation errors $\boldsymbol{\delta\tilde{J}}$ in the Taylor expansion series of the deformation gradients. We calculate $\boldsymbol{\delta\tilde{J}}_A - \boldsymbol{\delta\tilde{J}}_K$ for the strain-dependent elements of the deformation gradients $\tilde{\boldsymbol{J}}_A - \tilde{\boldsymbol{J}}_K$, using Eqs. (9) and (10) and the exact formulas listed in Table II. In Fig. 3, we show the elements of $\boldsymbol{\delta\tilde{J}}_C - \boldsymbol{\delta\tilde{J}}_J$, obtained for $\eta = \eta_{\max}$, as a function of the degree of the Taylor polynomial m. The results for the diagonal elements of $\boldsymbol{\delta\tilde{J}}_A$, $\boldsymbol{\delta\tilde{J}}_B$, and $\boldsymbol{\delta\tilde{J}}_K$ are the same as for the element $\delta\tilde{J}_{C,11}$ shown in Fig. 3(a). As expected, all strain-dependent elements of $\boldsymbol{\delta\tilde{J}}_C - \boldsymbol{\delta\tilde{J}}_J$ decrease with increasing m. Interestingly, for a given m, the nondiagonal elements of $\boldsymbol{\delta\tilde{J}}_C - \boldsymbol{\delta\tilde{J}}_J$ are larger than the diagonal ones. This applies particularly to $\delta\tilde{J}_{E,12}$, $\delta\tilde{J}_{F,12}$, $\delta\tilde{J}_{H,12}$, $\delta\tilde{J}_{I,23}$, $\delta\tilde{J}_{J,12}$, and $\delta\tilde{J}_{J,23}$ which, for a given m, are approximately one order of magnitude larger than the other

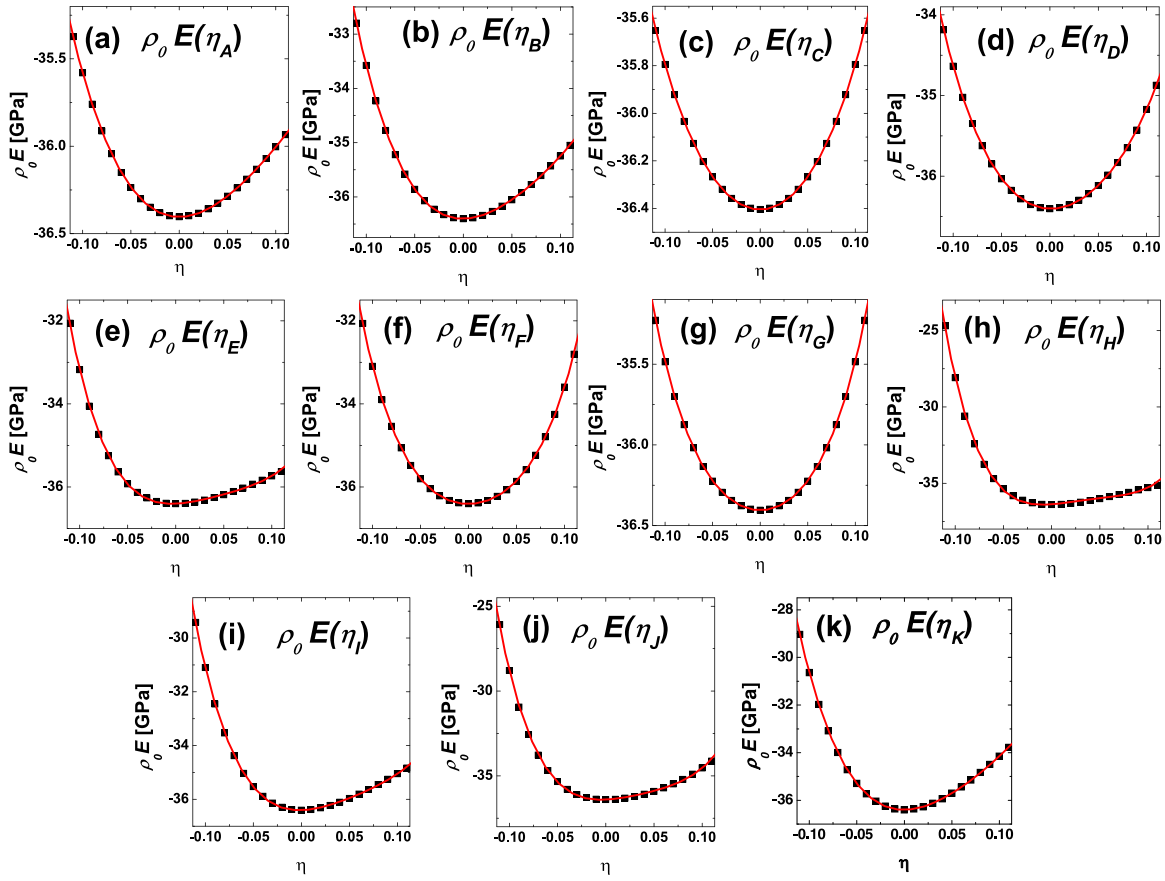

FIG. 1. The free-energy density $\rho_0 E$ as a function of the parameter η for the types of deformations used in the strain-energy method (Table III). Symbols correspond to the calculated *ab initio* data while the solid lines represent the fourth-order polynomial fits. For a clear illustration of the *ab initio* results, every fourth computed data point is shown.

TABLE IV. The FOECs (a), and the SOECs and TOECs (b), calculated for fcc Al using the strain-energy and strain-stress methods. The SOECs and the TOECs are obtained by the approximation of least squares (Appendix B). Experimental results and other theoretical calculations are also shown. The unit is in GPa.

C_{1111}	C_{1112}	C_{1122}	C_{1144}	C_{1155}	C_{4444}	C_{4455}	C_{1266}	C_{1255}	C_{1456}	C_{1123}
					(a)					
10327[a]	2978[a]	3589[a]	−680[a]	4620[a]	3885[a]	180[a]	6465[a]	87[a]	410[a]	−1043[a]
8750[b]	2989[b]	3951[b]	−585[b]	4683[b]	3918[b]	198[b]	4193[b]	95[b]	249[b]	−1051[b]
9916[c]	2656[c]	3708[c]	−578[c]	3554[c]	3329[c]	127[c]	4309[c]	−91[c]	148[c]	−1000[c]
	C_{11}	C_{12}	C_{44}	C_{111}	C_{112}	C_{144}	C_{155}	C_{456}	C_{123}	
					(b)					
	107.0[a]	59.0[a]	33.1[a]	−937[a]	−618[a]	69[a]	−738[a]	−29[a]	517[a]	
	114.3[b]	59.0[b]	33.4[b]	−1344[b]	−471[b]	22[b]	−578[b]	−40[b]	−57[b]	
	110.4[c]	54.5[c]	31.3[c]	−1253[c]	−426[c]	−12[c]	−493[c]	−21[c]	153[c]	
	106.8[d]	60.4[d]	28.3[d]	−1076[d]	−315[d]	−23[d]	−340[d]	−30[d]	36[d]	
	114.0[f]	62.0[f]	31.4[f]	−1224[e]	−373[e]	−64[e]	−368[e]	−27[e]	25[e]	
				−1427[f]	−408[f]	−85[f]	−396[f]	−42[f]	32[f]	

[a]This work, the strain-energy method.
[b]This work, the strain-stress method.
[c]Reference [15], the strain-energy method.
[d]Reference [32], experimental results (at 298 K).
[e]Reference [33], experimental results (at 298 K).
[f]Reference [34], experimental results (at 80 K).

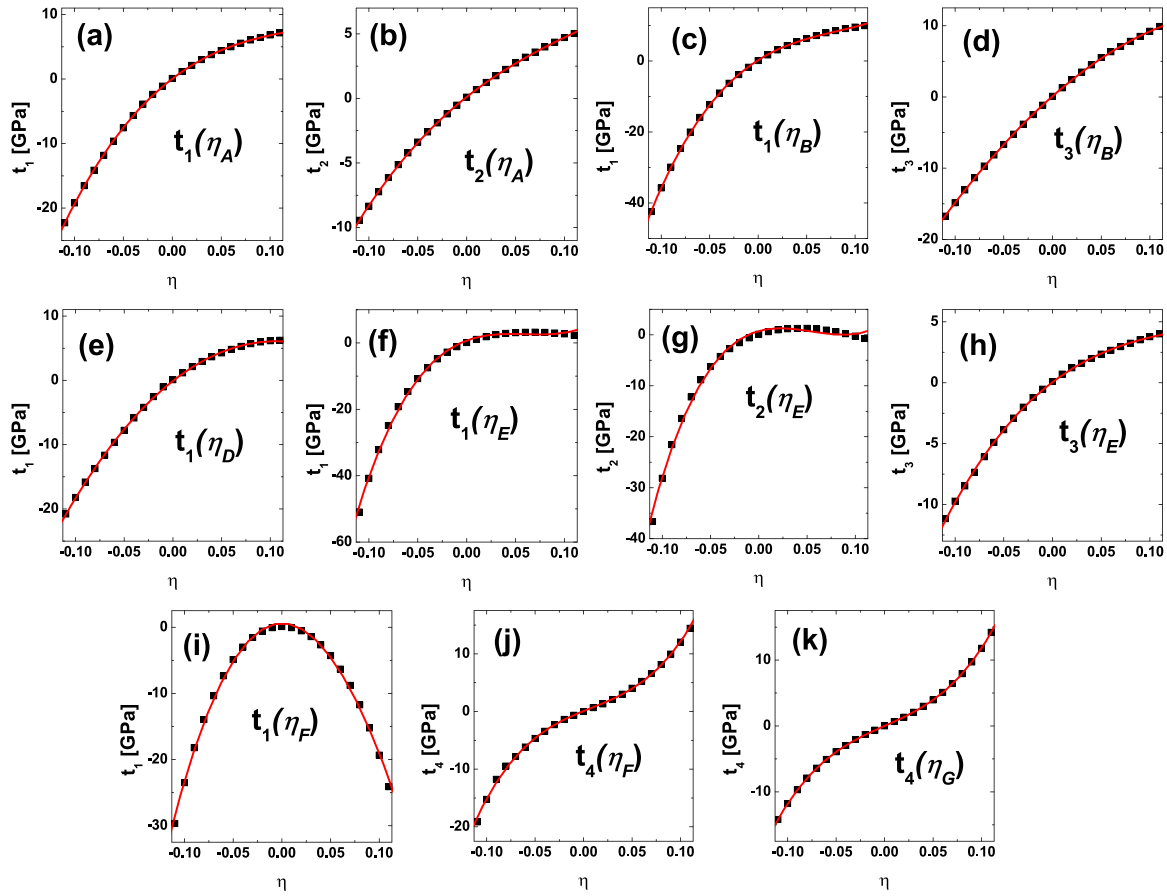

FIG. 2. The selected elements of the tensors $\boldsymbol{t}$ as functions of the parameter η for the types of deformations used in the strain-stress method (Table III). Symbols correspond to the calculated *ab initio* data while the solid lines represent the third-order polynomial fits. For a clear illustration of the *ab initio* results, every fourth computed data point is shown.

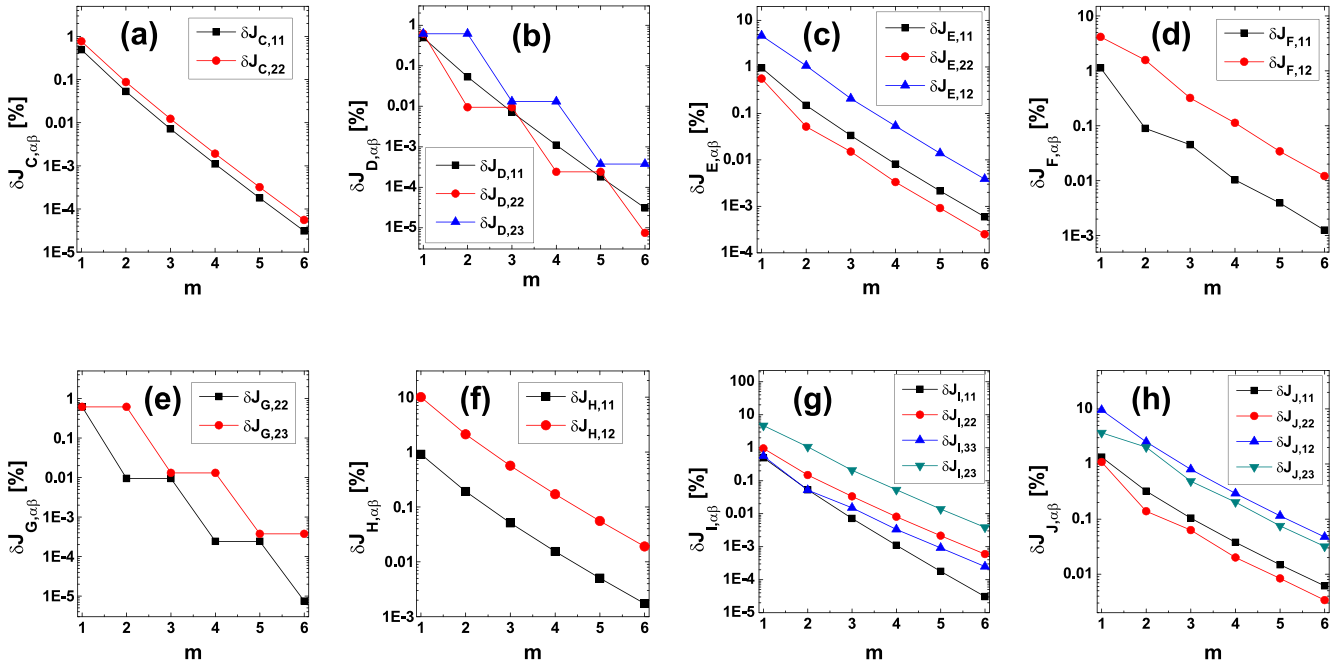

FIG. 3. The truncation errors, $\boldsymbol{\delta\tilde{J}}_C - \boldsymbol{\delta\tilde{J}}_J$, in the Taylor expansion series of the deformation gradients $\tilde{\boldsymbol{J}}_C - \tilde{\boldsymbol{J}}_J$, obtained for $\eta = \eta_{\max}$, as a function of m.

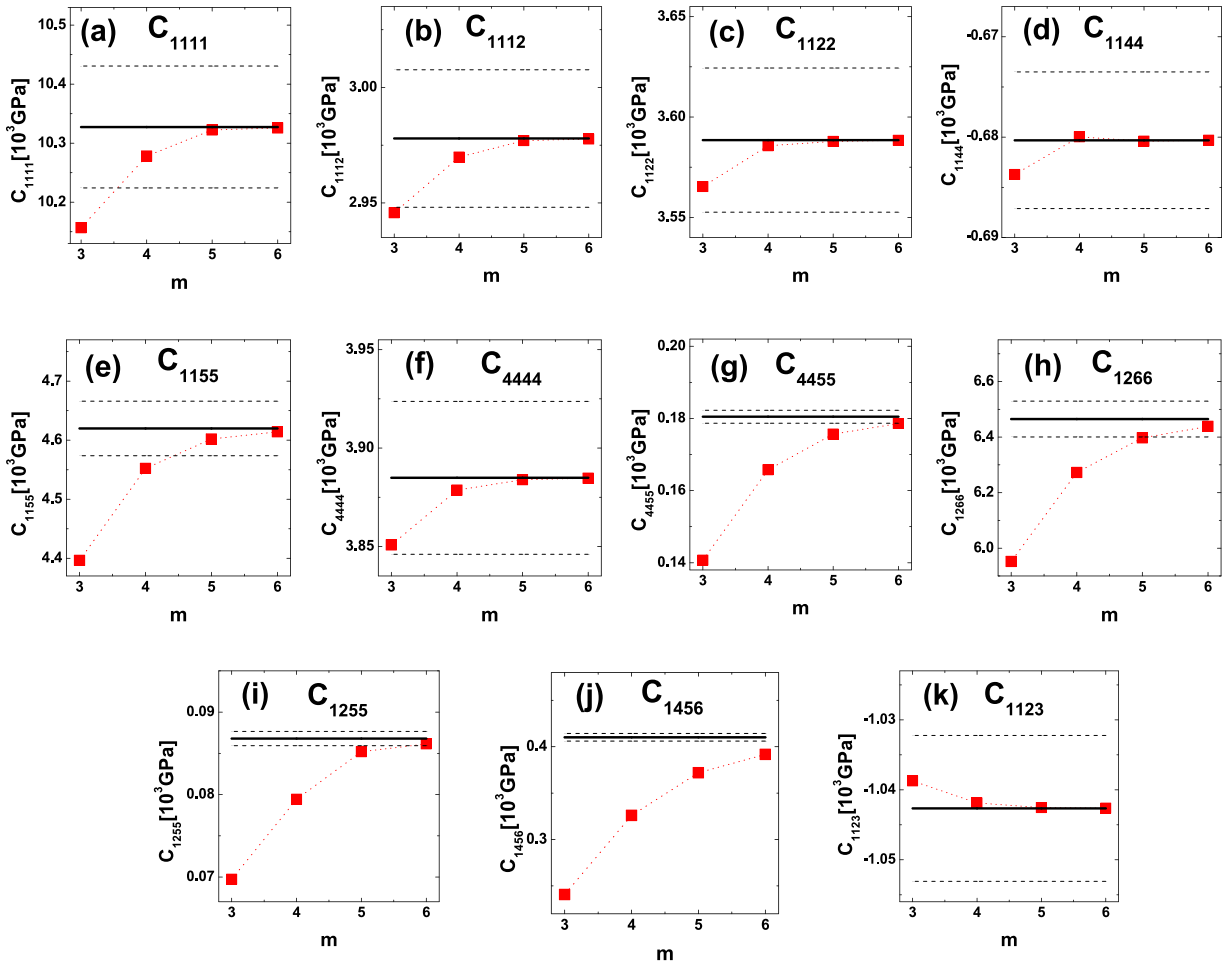

FIG. 4. The FOECs obtained using the strain-energy method with the deformation gradients $\tilde{\boldsymbol{J}}_A - \tilde{\boldsymbol{J}}_K$ approximated by their mth-degree Taylor polynomials (squares) as a function of m. The results obtained using the exact $\tilde{\boldsymbol{J}}_A - \tilde{\boldsymbol{J}}_K$ tensors are represented by the solid lines while the dashed lines illustrate a tolerance of 1% error.

elements of $\delta\tilde{\boldsymbol{J}}_C - \delta\tilde{\boldsymbol{J}}_J$. Note that for $m = 6$, all elements of $\delta\tilde{\boldsymbol{J}}_C - \delta\tilde{\boldsymbol{J}}_J$ are smaller than 0.1%.

In Fig. 4, we present the FOECs (squares) obtained using the strain-energy method with the deformation gradients $\tilde{\boldsymbol{J}}_A - \tilde{\boldsymbol{J}}_K$ approximated by their mth-degree Taylor polynomials. The results obtained using the exact $\tilde{\boldsymbol{J}}_A - \tilde{\boldsymbol{J}}_K$ tensors are represented by the solid lines while the dashed lines illustrate tolerance of 1% error. As expected, all FOECs obtained using the Taylor polynomials converge to the results obtained using the exact $\tilde{\boldsymbol{J}}$ tensors. We observe that C_{1122}, C_{1144}, C_{4444}, and C_{1123} are already within tolerance of 1% error for $m = 3$. For C_{1111} and C_{1112}, one needs $m = 4$ to achieve the desired tolerance. The C_{1155} and C_{1266} elastic constants are within relative errors of 1% for $m = 5$, while C_{4455} and C_{1255} reach these limits for $m = 6$. For C_{1456}, even $m = 6$ is not sufficient to get the result within tolerance of 1% error. The requirement of larger values of the m parameter for C_{1155}, C_{1266}, C_{4455}, C_{1255}, and C_{1456} originates from significant values of the nondiagonal elements of $\delta\tilde{\boldsymbol{J}}_E$, $\delta\tilde{\boldsymbol{J}}_F$, $\delta\tilde{\boldsymbol{J}}_H$, $\delta\tilde{\boldsymbol{J}}_I$, and $\delta\tilde{\boldsymbol{J}}_J$.

In Fig. 5, we show the FOECs obtained using the strain-stress method with the deformation gradients $\tilde{\boldsymbol{J}}_A - \tilde{\boldsymbol{J}}_K$ approximated by their mth-degree Taylor polynomials (squares). Again, the results obtained using the exact $\tilde{\boldsymbol{J}}_A - \tilde{\boldsymbol{J}}_K$ tensors are represented by the solid lines while the dashed lines illustrate tolerance of 1% error. Like in the case of the strain-energy method, all FOECs obtained using the Taylor polynomials converge to the results obtained using the exact $\tilde{\boldsymbol{J}}$ tensors, as expected. The deviations of the FOECs, caused by the truncation of the Taylor expansion series of the deformation gradients, are smaller for the strain-stress method than the strain-energy approach and thus, in the former case, smaller values of the m parameter are needed to get the results within relative errors of 1%. One can see that C_{1111}, C_{1112}, C_{1122}, C_{1144}, C_{4444}, and C_{1123} are already within tolerance of 1% error for $m = 3$. To achieve the desired tolerance, one needs $m = 4$ for C_{1155} and C_{1266}, $m = 5$ for C_{4455} and C_{1255}, and $m = 6$ for C_{1456}. The requirement of larger values of the m parameter for C_{1155}, C_{1266}, C_{4455}, C_{1255}, and C_{1456} originates again from significant values of the nondiagonal elements of $\delta\tilde{\boldsymbol{J}}_E$, $\delta\tilde{\boldsymbol{J}}_F$, $\delta\tilde{\boldsymbol{J}}_H$, $\delta\tilde{\boldsymbol{J}}_I$, and $\delta\tilde{\boldsymbol{J}}_J$.

IV. CONCLUSIONS

We have presented a general and easy-to-use method of the *ab initio* calculation of the HOECs, which is based on the analytical formulas for the deformation-gradient tensors

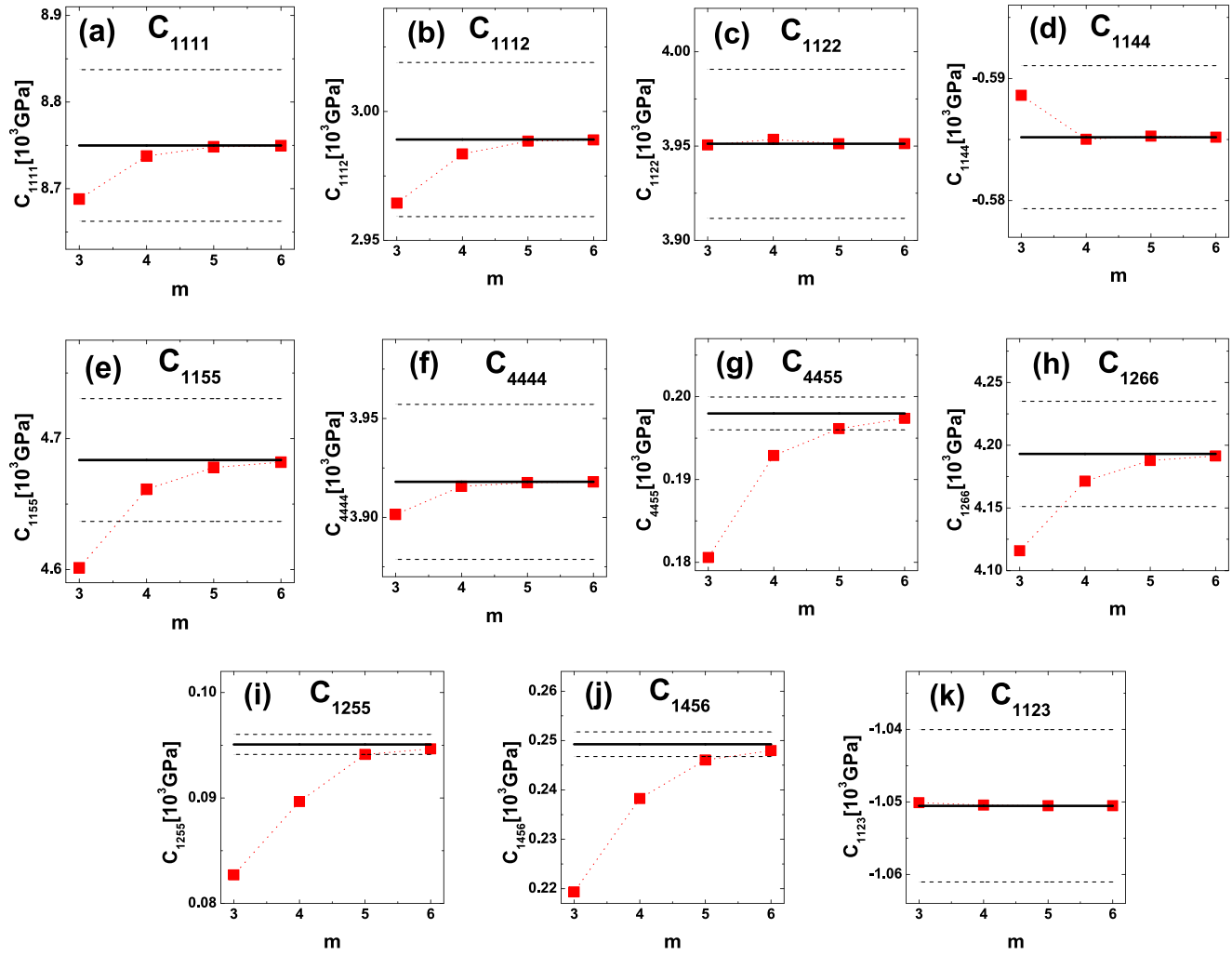

FIG. 5. The FOECs obtained using the strain-stress method with the deformation gradients $\tilde{\boldsymbol{J}}_A - \tilde{\boldsymbol{J}}_K$ approximated by their mth-degree Taylor polynomials (squares) as a function of m. The results obtained using the exact $\tilde{\boldsymbol{J}}_A - \tilde{\boldsymbol{J}}_K$ tensors are represented by the solid lines while the dashed lines illustrate a tolerance of 1% error.

as functions of the Lagrangian strain. The method allows for elimination of the truncation errors in the Taylor expansion series of the deformation gradients and is particularly useful to calculate the FOECs, where large strains have to be applied. It also facilitates the calculation of the Lagrangian stress, which is helpful in the implementation of the strain-stress method. To demonstrate the application of our approach, we have derived the analytic formulas for the deformation gradients as functions of the Lagrangian strain tensors, which are used in calculations of the TOECs in trigonal crystals and the FOECs in cubic crystals. Then, we have performed the *ab initio* calculations of the FOECs in fcc Al. We have discussed the results obtained using the strain-energy and strain-stress methods and analyzed the errors of the FOECs which would be incurred when approximating the deformation gradients by the Taylor polynomials. We have shown that the relatively small truncation errors in the Taylor expansion series of the deformation gradients can cause significant deviations of the FOECs, which makes our exact analytical formulas for the deformation gradients important. This effect is larger for the strain-energy method than for the strain-stress approach. In both methods, the deviations are particularly significant for the C_{1155}, C_{1266}, C_{4455}, C_{1255}, and C_{1456} elastic constants and are mainly caused by the truncation errors in the nondiagonal elements of the Taylor expansion series of the deformation gradients.

ACKNOWLEDGMENTS

The author would like to thank G. Rządkowski from the Faculty of Management, Warsaw University of Technology for help with the matrix calculations. He also wishes to acknowledge useful discussions with P. Kempisty, M. Wierzbowska, and J. Piechota from the IHPP PAS concerning the *ab initio* calculations using the VASP package. The *ab initio* calculations were carried out with the support of the Interdisciplinary Centre for Mathematical and Computational Modelling at the University of Warsaw (ICM UW) (Grant No. GB75-8).

APPENDIX A

Below, we present the $\boldsymbol{S}$ matrices in terms of the elements of the $\tilde{\boldsymbol{J}}$ tensors. They have been obtained for six types of deformations, i.e., η_A, η_B, η_D, η_E, η_F, and η_G (see Tables II and III), which we have used to calculate the FOECs applying

TABLE V. The third- and the second-degree coefficients in the strain-energy relation [Eq. (3)] for the types of the strain tensors, which have been used in Sec. III to determine the FOECs in cubic crystals.

Strain types	Third-degree coefficients in the strain-energy relation	Second-degree coefficients in the strain-energy relation
$\boldsymbol{\eta}_A = (\eta, 0, 0, 0, 0, 0)$	$A = \frac{1}{6}C_{111}$	$A' = \frac{1}{2}C_{11}$
$\boldsymbol{\eta}_B = (\eta, \eta, 0, 0, 0, 0)$	$B = \frac{1}{3}C_{111} + C_{112}$	$B' = C_{11} + C_{12}$
$\boldsymbol{\eta}_C = (\eta, -\eta, 0, 0, 0, 0)$	$C = 0$	$C' = C_{11} - C_{12}$
$\boldsymbol{\eta}_D = (\eta, 0, 0, 2\eta, 0, 0)$	$D = \frac{1}{6}C_{111} + 2C_{144}$	$D' = \frac{1}{2}C_{11} + 2C_{44}$
$\boldsymbol{\eta}_E = (\eta, 0, 0, 0, 0, 2\eta)$	$E = \frac{1}{6}C_{111} + 2C_{155}$	$E' = \frac{1}{2}C_{11} + 2C_{44}$
$\boldsymbol{\eta}_F = (0, 0, 0, 2\eta, 2\eta, 2\eta)$	$F = 8C_{456}$	$F' = 6C_{44}$
$\boldsymbol{\eta}_G = (0, 0, 0, 2\eta, 0, 0)$	$G = 0$	$G' = 2C_{44}$
$\boldsymbol{\eta}_H = (\eta, \eta, 0, 0, 0, 2\eta)$	$H = \frac{1}{3}C_{111} + C_{112} + 4C_{155}$	$H' = C_{11} + C_{12} + 2C_{44}$
$\boldsymbol{\eta}_I = (\eta, \eta, 0, 2\eta, 0, 0)$	$I = \frac{1}{3}C_{111} + C_{112} + 2C_{144} + 2C_{155}$	$I' = C_{11} + C_{12} + 2C_{44}$
$\boldsymbol{\eta}_J = (\eta, 0, 0, 2\eta, 2\eta, 2\eta)$	$J = \frac{1}{6}C_{111} + 2C_{144} + 4C_{155} + 8C_{456}$	$J' = \frac{1}{2}C_{11} + 6C_{44}$
$\boldsymbol{\eta}_K = (\eta, \eta, \eta, 0, 0, 0)$	$K = \frac{1}{2}C_{111} + 3C_{112} + C_{123}$	$K' = \frac{3}{2}C_{11} + 3C_{12}$

the strain-stress approach:

$$S_A = \begin{bmatrix} a & 0 & 0 & 0 & 0 & 0 \\ 0 & b & 0 & 0 & 0 & 0 \\ 0 & 0 & b & 0 & 0 & 0 \\ 0 & 0 & 0 & b & 0 & 0 \\ 0 & 0 & 0 & 0 & 1 & 0 \\ 0 & 0 & 0 & 0 & 0 & 1 \end{bmatrix}, \tag{A1}$$

where $a = \frac{1}{\tilde{J}_{A,11}}$ and $b = \tilde{J}_{A,11}$;

$$S_B = \begin{bmatrix} 1 & 0 & 0 & 0 & 0 & 0 \\ 0 & 1 & 0 & 0 & 0 & 0 \\ 0 & 0 & a & 0 & 0 & 0 \\ 0 & 0 & 0 & b & 0 & 0 \\ 0 & 0 & 0 & 0 & b & 0 \\ 0 & 0 & 0 & 0 & 0 & 1 \end{bmatrix}, \tag{A2}$$

where $a = (\tilde{J}_{B,11})^2$ and $b = \tilde{J}_{B,11}$;

$$S_D = \begin{bmatrix} a & 0 & 0 & 0 & 0 & 0 \\ 0 & b & c & 2e & 0 & 0 \\ 0 & c & b & 2e & 0 & 0 \\ 0 & e & e & d & 0 & 0 \\ 0 & 0 & 0 & 0 & f & g \\ 0 & 0 & 0 & 0 & g & f \end{bmatrix}, \tag{A3}$$

where $a = \frac{(\tilde{J}_{D,22})^2 - (\tilde{J}_{D,23})^2}{\tilde{J}_{D,11}}$, $b = \frac{\tilde{J}_{D,11}(\tilde{J}_{D,22})^2}{(\tilde{J}_{D,22})^2 - (\tilde{J}_{D,23})^2}$, $c = \frac{\tilde{J}_{D,11}(\tilde{J}_{D,23})^2}{(\tilde{J}_{D,22})^2 - (\tilde{J}_{D,23})^2}$, $d = \frac{\tilde{J}_{D,11}[(\tilde{J}_{D,22})^2 + (\tilde{J}_{D,23})^2]}{(\tilde{J}_{D,22})^2 - (\tilde{J}_{D,23})^2}$, $e = \frac{-\tilde{J}_{D,11}\tilde{J}_{D,22}\tilde{J}_{D,23}}{(\tilde{J}_{D,22})^2 - (\tilde{J}_{D,23})^2}$, $f = \tilde{J}_{D,22}$ and $g = -\tilde{J}_{D,23}$;

$$S_E = \begin{bmatrix} a & c & 0 & 0 & 0 & 2i \\ c & b & 0 & 0 & 0 & 2j \\ 0 & 0 & d & 0 & 0 & 0 \\ 0 & 0 & 0 & e & g & 0 \\ 0 & 0 & 0 & g & f & 0 \\ i & j & 0 & 0 & 0 & h \end{bmatrix}, \tag{A4}$$

where $a = \frac{(\tilde{J}_{E,22})^2}{\tilde{J}_{E,11}\tilde{J}_{E,22} - (\tilde{J}_{E,12})^2}$, $b = \frac{(\tilde{J}_{E,11})^2}{\tilde{J}_{E,11}\tilde{J}_{E,22} - (\tilde{J}_{E,12})^2}$, $c = \frac{(\tilde{J}_{E,12})^2}{\tilde{J}_{E,11}\tilde{J}_{E,22} - (\tilde{J}_{E,12})^2}$, $d = \tilde{J}_{E,11}\tilde{J}_{E,22} - (\tilde{J}_{E,12})^2$, $e = \tilde{J}_{E,11}$, $f = \tilde{J}_{E,22}$, $g = -\tilde{J}_{E,12}$, $h = \frac{\tilde{J}_{E,11}\tilde{J}_{E,22} + (\tilde{J}_{E,12})^2}{\tilde{J}_{E,11}\tilde{J}_{E,22} - (\tilde{J}_{E,12})^2}$, $i = \frac{-\tilde{J}_{E,12}\tilde{J}_{E,22}}{\tilde{J}_{E,11}\tilde{J}_{E,22} - (\tilde{J}_{E,12})^2}$ and $j = \frac{-\tilde{J}_{E,11}\tilde{J}_{E,12}}{\tilde{J}_{E,11}\tilde{J}_{E,22} - (\tilde{J}_{E,12})^2}$;

$$S_F = \begin{bmatrix} a & b & b & 2b & 2c & 2c \\ b & a & b & 2c & 2b & 2c \\ b & b & a & 2c & 2c & 2b \\ b & c & c & d & e & e \\ c & b & c & e & d & e \\ c & c & b & e & e & d \end{bmatrix}, \tag{A5}$$

where $a = \frac{(\tilde{J}_{F,11} + \tilde{J}_{F,12})^2}{\tilde{J}_{F,11} + 2\tilde{J}_{F,12}}$, $b = \frac{(\tilde{J}_{F,12})^2}{\tilde{J}_{F,11} + 2\tilde{J}_{F,12}}$, $c = \frac{-\tilde{J}_{F,12}(\tilde{J}_{F,11} + \tilde{J}_{F,12})}{\tilde{J}_{F,11} + 2\tilde{J}_{F,12}}$, $d = \frac{(\tilde{J}_{F,11} + \tilde{J}_{F,12})^2 + (\tilde{J}_{F,12})^2}{\tilde{J}_{F,11} + 2\tilde{J}_{F,12}}$ and $e = \frac{-\tilde{J}_{F,11}\tilde{J}_{F,12}}{\tilde{J}_{F,11} + 2\tilde{J}_{F,12}}$;

$$S_G = \begin{bmatrix} a & 0 & 0 & 0 & 0 & 0 \\ 0 & b & c & 2e & 0 & 0 \\ 0 & c & b & 2e & 0 & 0 \\ 0 & e & e & d & 0 & 0 \\ 0 & 0 & 0 & 0 & f & g \\ 0 & 0 & 0 & 0 & g & f \end{bmatrix}, \tag{A6}$$

where $a = (\tilde{J}_{G,22})^2 - (\tilde{J}_{G,23})^2$, $b = \frac{(\tilde{J}_{G,22})^2}{(\tilde{J}_{G,22})^2 - (\tilde{J}_{G,23})^2}$, $c = \frac{(\tilde{J}_{G,23})^2}{(\tilde{J}_{G,22})^2 - (\tilde{J}_{G,23})^2}$, $d = \frac{[(\tilde{J}_{G,22})^2 + (\tilde{J}_{G,23})^2]}{(\tilde{J}_{G,22})^2 - (\tilde{J}_{G,23})^2}$, $e = \frac{-\tilde{J}_{G,22}\tilde{J}_{G,23}}{(\tilde{J}_{G,22})^2 - (\tilde{J}_{G,23})^2}$, $f = \tilde{J}_{G,22}$, and $g = -\tilde{J}_{G,23}$.

Note that using the analytical formulas for the tensors $\tilde{\boldsymbol{J}}_A$, $\tilde{\boldsymbol{J}}_B$, $\tilde{\boldsymbol{J}}_D$, $\tilde{\boldsymbol{J}}_E$, $\tilde{\boldsymbol{J}}_F$, and $\tilde{\boldsymbol{J}}_G$, taken from Table II, one can express the elements of the above $\boldsymbol{S}$ matrices as functions of one parameter $\eta \in \langle -\eta_{\max}, \eta_{\max} \rangle$, which is convenient from the computational point of view.

TABLE VI. The second- and the first-degree coefficients in the strain-stress relations [Eq. (4)] for the types of the strain tensors, which have been used in Sec. III to determine the FOECs in cubic crystals.

Strain types	Second-degree coefficients in the strain-stress relation	First-degree coefficients in the strain-stress relation
$\boldsymbol{\eta}_A = (\eta, 0, 0, 0, 0, 0)$	$t_1(\eta):\ A = \frac{1}{2}C_{111}$	$t_1(\eta):\ A' = C_{11}$
	$t_2(\eta):\ B = \frac{1}{2}C_{112}$	$t_2(\eta):\ B' = C_{12}$
$\boldsymbol{\eta}_B = (\eta, \eta, 0, 0, 0, 0)$	$t_1(\eta):\ C = \frac{1}{2}C_{111} + \frac{3}{2}C_{112}$	$t_1(\eta):\ C' = C_{11} + C_{12}$
	$t_3(\eta):\ D = \frac{1}{2}C_{112} + C_{123}$	$t_3(\eta):\ D' = 2C_{12}$
$\boldsymbol{\eta}_D = (\eta, 0, 0, 2\eta, 0, 0)$	$t_1(\eta):\ E = \frac{1}{2}C_{111} + 2C_{144}$	$t_1(\eta):\ E' = C_{11}$
$\boldsymbol{\eta}_E = (\eta, 0, 0, 0, 0, 2\eta)$	$t_1(\eta):\ F = \frac{1}{2}C_{111} + 2C_{155}$	$t_1(\eta):\ F' = C_{11}$
	$t_2(\eta):\ G = \frac{1}{2}C_{112} + 2C_{155}$	$t_2(\eta):\ G' = C_{12}$
	$t_3(\eta):\ H = \frac{1}{2}C_{112} + 2C_{144}$	$t_3(\eta):\ H' = C_{12}$
$\boldsymbol{\eta}_F = (0, 0, 0, 2\eta, 2\eta, 2\eta)$	$t_1(\eta):\ I = 2C_{144} + 4C_{155}$	$t_1(\eta):\ I' = 0$
	$t_4(\eta):\ J = 4C_{456}$	$t_4(\eta):\ J' = 2C_{44}$
$\boldsymbol{\eta}_G = (0, 0, 0, 2\eta, 0, 0)$	$t_4(\eta):\ K = 0$	$t_4(\eta):\ K' = 2C_{44}$

APPENDIX B:

In order to obtain the TOECs and the SOECs from the strain-energy and strain-stress dependencies calculated for determination of the FOECs (Figs. 1 and 2), we apply the method of least squares. In Table V, we present the third- and the second-degree coefficients in the strain-energy relation [Eq. (3)] for the types of the strain tensors which have been used in Sec. III to determine the FOECs. These coefficients are expressed by the linear combinations of the TOECs and the SOECs, respectively. In Table VI we show the second- and the first-degree coefficients in the strain-stress relations

TABLE VII. The coefficients obtained using the method of least squares for the TOECs and the SOECs in the strain-energy and the strain-stress approaches.

	a	b	c	d	e	f	g	h	i	j	k
C_{111}	$\left(\frac{118}{41}\right)^a$	$\left(\frac{56}{41}\right)^a$	0^a	$\left(\frac{52}{41}\right)^a$	$\left(\frac{84}{41}\right)^a$	$\left(\frac{8}{41}\right)^a$	0^a	$\left(\frac{-12}{41}\right)^a$	$\left(\frac{-44}{41}\right)^a$	$\left(\frac{-8}{41}\right)^a$	0^a
	$\left(\frac{163}{248}\right)^b$	$\left(\frac{-37}{248}\right)^b$	$\left(\frac{13}{62}\right)^b$	0^b	$\left(\frac{127}{248}\right)^b$	$\left(\frac{77}{124}\right)^b$	$\left(\frac{-23}{124}\right)^b$	$\left(\frac{-73}{248}\right)^b$	$\left(\frac{-27}{124}\right)^b$	0^b	0^b
C_{112}	$\left(\frac{-30}{41}\right)^a$	$\left(\frac{8}{41}\right)^a$	0^a	$\left(\frac{-16}{41}\right)^a$	$\left(\frac{-29}{41}\right)^a$	$\left(\frac{7}{41}\right)^a$	0^a	$\left(\frac{10}{41}\right)^a$	$\left(\frac{23}{41}\right)^a$	$\left(\frac{-7}{41}\right)^a$	0^a
	$\left(\frac{-37}{248}\right)^b$	$\left(\frac{51}{248}\right)^b$	$\left(\frac{29}{62}\right)^b$	0^b	$\left(\frac{-41}{248}\right)^b$	$\left(\frac{-19}{124}\right)^b$	$\left(\frac{25}{124}\right)^b$	$\left(\frac{47}{248}\right)^b$	$\left(\frac{-3}{124}\right)^b$	0^b	0^b
C_{144}	$\left(\frac{-11}{82}\right)^a$	$\left(\frac{-4}{41}\right)^a$	0^a	$\left(\frac{8}{41}\right)^a$	$\left(\frac{-6}{41}\right)^a$	$\left(\frac{-7}{82}\right)^a$	0^a	$\left(\frac{-5}{41}\right)^a$	$\left(\frac{9}{41}\right)^a$	$\left(\frac{7}{82}\right)^a$	0^a
	$\left(\frac{-9}{248}\right)^b$	$\left(\frac{-1}{248}\right)^b$	$\left(\frac{-3}{62}\right)^b$	0^b	$\left(\frac{47}{248}\right)^b$	$\left(\frac{-13}{124}\right)^b$	$\left(\frac{-9}{124}\right)^b$	$\left(\frac{55}{248}\right)^b$	$\left(\frac{11}{124}\right)^b$	0^b	0^b
C_{155}	$\left(\frac{-17}{246}\right)^a$	$\left(\frac{-31}{246}\right)^a$	0^a	$\left(\frac{-10}{123}\right)^a$	$\left(\frac{15}{246}\right)^a$	$\left(\frac{-11}{123}\right)^a$	0^a	$\left(\frac{11}{82}\right)^a$	$\left(\frac{-1}{123}\right)^a$	$\left(\frac{11}{123}\right)^a$	0^a
	$\left(\frac{-9}{992}\right)^b$	$\left(\frac{-1}{992}\right)^b$	$\left(\frac{-3}{248}\right)^b$	0^b	$\left(\frac{-77}{992}\right)^b$	$\left(\frac{49}{496}\right)^b$	$\left(\frac{53}{496}\right)^b$	$\left(\frac{-69}{992}\right)^b$	$\left(\frac{73}{496}\right)^b$	0^b	0^b
C_{456}	$\left(\frac{1}{246}\right)^a$	$\left(\frac{29}{984}\right)^a$	0^a	$\left(\frac{-17}{984}\right)^a$	$\left(\frac{-3}{164}\right)^a$	$\left(\frac{23}{246}\right)^a$	0^a	$\left(\frac{-15}{984}\right)^a$	$\left(\frac{-7}{492}\right)^a$	$\left(\frac{31}{984}\right)^a$	0^a
	0^b	0^b	0^b	0^b	0^b	0^b	0^b	0^b	0^b	$\left(\frac{1}{4}\right)^b$	0^b
C_{123}	$\left(\frac{31}{41}\right)^a$	$\left(\frac{-52}{41}\right)^a$	0^a	$\left(\frac{22}{41}\right)^a$	$\left(\frac{45}{41}\right)^a$	$\left(\frac{-25}{41}\right)^a$	0^a	$\left(\frac{-24}{41}\right)^a$	$\left(\frac{-47}{41}\right)^a$	$\left(\frac{25}{41}\right)^a$	1^a
	$\left(\frac{37}{496}\right)^b$	$\left(\frac{-51}{496}\right)^b$	$\left(\frac{-29}{124}\right)^b$	1^b	$\left(\frac{41}{496}\right)^b$	$\left(\frac{19}{248}\right)^b$	$\left(\frac{-25}{248}\right)^b$	$\left(\frac{-47}{496}\right)^b$	$\left(\frac{3}{248}\right)^b$	0^b	0^b
C_{11}	$\left(\frac{590}{4083}\right)^a$	$\left(\frac{206}{1361}\right)^a$	$\left(\frac{1742}{4083}\right)^a$	$\left(\frac{136}{1361}\right)^a$	$\left(\frac{136}{1361}\right)^a$	$\left(\frac{-182}{1361}\right)^a$	$\left(\frac{-182}{4083}\right)^a$	$\left(\frac{436}{4083}\right)^a$	$\left(\frac{436}{4083}\right)^a$	$\left(\frac{44}{4083}\right)^a$	$\left(\frac{28}{1361}\right)^a$
	$\left(\frac{8}{31}\right)^b$	$\left(\frac{-1}{31}\right)^b$	$\left(\frac{7}{31}\right)^b$	$\left(\frac{-2}{31}\right)^b$	$\left(\frac{8}{31}\right)^b$	$\left(\frac{8}{31}\right)^b$	$\left(\frac{-1}{31}\right)^b$	$\left(\frac{-1}{31}\right)^b$	0^b	0^b	0^b
C_{12}	$\left(\frac{-281}{4083}\right)^a$	$\left(\frac{8}{1361}\right)^a$	$\left(\frac{-1148}{4083}\right)^a$	$\left(\frac{-74}{1361}\right)^a$	$\left(\frac{-74}{1361}\right)^a$	$\left(\frac{59}{1361}\right)^a$	$\left(\frac{59}{4083}\right)^a$	$\left(\frac{83}{4083}\right)^a$	$\left(\frac{83}{4083}\right)^a$	$\left(\frac{-104}{4083}\right)^a$	$\left(\frac{305}{1361}\right)^a$
	$\left(\frac{-1}{31}\right)^b$	$\left(\frac{4}{31}\right)^b$	$\left(\frac{3}{31}\right)^b$	$\left(\frac{8}{31}\right)^b$	$\left(\frac{-1}{31}\right)^b$	$\left(\frac{-1}{31}\right)^b$	$\left(\frac{4}{31}\right)^b$	$\left(\frac{4}{31}\right)^b$	0^b	0^b	0^b
C_{44}	$\left(\frac{-91}{8166}\right)^a$	$\left(\frac{-41}{2722}\right)^a$	$\left(\frac{-241}{8166}\right)^a$	$\left(\frac{39}{2722}\right)^a$	$\left(\frac{39}{2722}\right)^a$	$\left(\frac{104}{1361}\right)^a$	$\left(\frac{104}{4083}\right)^a$	$\left(\frac{85}{8166}\right)^a$	$\left(\frac{85}{8166}\right)^a$	$\left(\frac{533}{8166}\right)^a$	$\left(\frac{-16}{1361}\right)^a$
	0^b	0^b	0^b	0^b	0^b	0^b	0^b	0^b	0^b	$\left(\frac{1}{4}\right)^b$	$\left(\frac{1}{4}\right)^b$

[a]The strain-energy method.
[b]The strain-stress method.

[Eq. (4)] for the types of the strain tensors which have been used to determine the FOECs. Again, these coefficients are expressed by the linear combinations of the TOECs and the SOECs, respectively. Since we have 11 linear combinations of the TOECs and also 11 linear combinations of the SOECs, we apply the method of least squares to obtain the approximated values of six TOECs and three SOECs. As a result, we get

$$C_{ijk} = aA + bB + cC + dD + eE + fF + gG + hH + iI + jJ + kK, \tag{B1}$$

$$C_{ij} = a\acute{A} + b\acute{B} + c\acute{C} + d\acute{D} + e\acute{E} + f\acute{F} + g\acute{G} + h\acute{H} + i\acute{I} + j\acute{J} + k\acute{K}, \tag{B2}$$

where the coefficients denoted by uppercase letters are shown in Tables V and VI while lowercase letters represent the coefficients listed in Table VII.

[1] D. C. Wallace, *Thermodynamics of Crystals* (Dover, New York, 1998).
[2] Y. Hiki, Annu. Rev. Mater. Sci. **11**, 51 (1981).
[3] G. A. Saunders, H. B. Senin, H. A. A. Sidek, and J. Pelzl, Phys. Rev. B. **48**, 15801 (1993).
[4] K. Brugger and T. C. Fritz, Phys. Rev. **157**, 524 (1967).
[5] J. Philip and M. A. Breazeale, J. Appl. Phys. **54**, 752 (1983).
[6] F. Birch, Phys. Rev. **71**, 809 (1947).
[7] J. Clayton, R. Kraft, and R. Leavy, Int. J. Solids Struct. **49**, 2686 (2012).
[8] M. de Jong, I. Winter, D. C. Chrzan, and M. Asta, Phys. Rev. B **96**, 014105 (2017).
[9] S. P. Łepkowski, Phys. Rev. B **78**, 153307 (2008).
[10] E. Cadelano, P. L. Palla, S. Giordano, and L. Colombo, Phys. Rev. Lett. **102**, 235502 (2009).
[11] X. Wang, Y. Gu, X. Sun, H. Wang, and Y. Zhang, J. Appl. Phys. **115**, 213516 (2014).
[12] S. P. Łepkowski and W. Bardyszewski, J. Phys.: Condens. Matter **29**, 055702 (2017).
[13] S. P. Łepkowski and W. Bardyszewski, J. Phys.: Condens. Matter **29**, 195702 (2017).
[14] G. Jurczak and P. Dłużewski, Comput. Mater. Sci. **111**, 197, (2016).
[15] H. Wang and M. Li, Phys. Rev. B **79**, 224102 (2009).
[16] Yu. Kh. Vekilov, O. M. Krasilnikov, A. V. Lugovskoy, and Yu. E. Lozovik, Phys. Rev. B **94**, 104114 (2016).
[17] O. M. Krasilnikov and Yu. Kh. Vekilov, Phys. Rev. B **100**, 134107 (2019).
[18] A. S. Johal and D. J. Dunstan, Phys. Rev. B **73**, 024106 (2006).
[19] J. M. Lang, Jr., and Y. M. Gupta, Phys. Rev. Lett. **106**, 125502 (2011).
[20] O. H. Nielsen and R. M. Martin, Phys. Rev. B **32**, 3780 (1985).
[21] M. Łopuszyński and J. A. Majewski, Phys. Rev. B **76**, 045202 (2007).
[22] J. Zhao, J. M. Winey, and Y. M. Gupta, Phys. Rev. B **75**, 094105 (2007).
[23] R. Wang, S. Wang, X. Wu, Y. Yao, and A. Liu, Intermetallics **18**, 2472 (2010).
[24] I. Mosyagin, A. V. Lugovskoy, O. M. Krasilnikov, Yu. Kh. Velikov, and S. I. Simak, Comput. Phys. Commun. **220**, 20 (2017).
[25] C. Wang, J. Gu, W. Zhang, B. Sun, D. Liu, and G. Liu, Comput. Mater. Sci. **124**, 375, (2016).
[26] A. Hmiel, J. M. Winey, Y. M. Gupta, and M. P. Desjarlais, Phys. Rev. B **93**, 174113 (2016).
[27] T. Cao, D. Cuffari, and A. Bongiorno, Phys. Rev. Lett. **121**, 216001 (2018).
[28] D. S. P. Tanner, M. A. Caro, S. Schulz, and E. P. O'Reilly, Phys. Rev. Mater. **3**, 013604 (2019).
[29] G. Kresse and J. Furthmuller, Phys. Rev. B **54**, 11169 (1996).
[30] G. Kresse and D. Joubert, Phys. Rev. B **59**, 1758 (1999).
[31] J. P. Perdew, K. Burke, and M. Ernzerhof, Phys. Rev. Lett. **77**, 3865 (1996).
[32] J. F. Thomas, Jr., Phys. Rev. **175**, 955 (1968).
[33] V. P. N. Sarma and P. J. Reddy, Phys. Status Solidi A **10**, 563 (1972).
[34] V. P. N. Sarma and P. J. Reddy, J. Phys. Chem. Solids **34**, 1593 (1973).